ORIGINAL ARTICLE

Decomposition of methane over alumina supported Fe and Ni–Fe bimetallic catalyst: Effect of preparation procedure and calcination temperature

A.S. Al-Fatesh [a,*], A.H. Fakeeha [a,*], A.A. Ibrahim [a], W.U. Khan [a], H. Atia [b], R. Eckelt [b], K. Seshan [c], B. Chowdhury [d]

[a] Chemical Engineering Department, College of Engineering, King Saud University, P.O. Box 800, Riyadh 11421, Saudi Arabia
[b] Leibniz Institute for Catalysis, Rostock, Germany
[c] University of Twente, PO Box 217, 7500 AE, Enschede, The Netherlands
[d] Department of Applied Chemistry, Indian School of Mines, Dhanbad, India

Abstract Catalytic decomposition of methane has been studied extensively as the production of hydrogen and formation of carbon nanotube is proven crucial from the scientific and technological point of view. In that context, variation of catalyst preparation procedure, calcination temperature and use of promoters could significantly alter the methane conversion, hydrogen yield and morphology of carbon nanotubes formed after the reaction. In this work, Ni promoted and unpromoted Fe/Al_2O_3 catalysts have been prepared by impregnation, sol–gel and co-precipitation method with calcination at two different temperatures. The catalysts were characterized by X-ray diffraction (XRD), N_2 physisorption, temperature programmed reduction (TPR) and thermogravimetric analysis (TGA) techniques. The catalytic activity was tested for methane decomposition reaction. The catalytic activity was high when calcined at 500 °C temperature irrespective of the preparation method. However while calcined at high temperature the catalyst prepared by impregnation method showed a high activity. It is found from XRD and TPR characterization that disordered iron oxides supported on alumina play an important role for dissociative chemisorptions of methane generating molecular hydrogen. The transmission electron microscope technique results of the spent catalysts showed the formation of carbon nanotube which is having length of 32–34 nm. The Fe nanoparticles are present on the tip of the carbon nanotube and nanotube grows by contraction–elongation mechanism. Among three different methodologies impregnation method was more effective to generate adequate active sites in the catalyst surface. The Ni promotion enhances the reducibility

* Corresponding authors. Tel.: +966 1 4676847; fax: +966 1 4678770.
E-mail address: anishf@ksu.edu.sa (A.S. Al-Fatesh).
Peer review under responsibility of King Saud University.

ELSEVIER **Production and hosting by Elsevier**

of Fe/Al$_2$O$_3$ oxides showing a higher catalytic activity. The catalyst is stable up to six hours on stream as observed in the activity results.

1. Introduction

The process of dehydrogenation of hydrocarbons over metal surface has many applications. Among them production of soot and carbon nanotubes (CNT) is an important outcome as revealed in literature [1]. There is continuous interest in the activation and decomposition of CH4 due to its importance in hydrogen production. An increasing concern on the environmental effects of energy use, in the form of global warming, ozone layer depletion, and acid rains has led to intense research on various forms of clean energy. Hydrogen is widely considered to be one of the most promising alternative energy carriers and clean fuel. Among several factors high yields in fuel cells, clean combustion without emission of CO$_2$, NO$_x$ or SO$_x$ are important from the perspective of renewable energy [1]. Traditionally, dry (with CO$_2$) reforming and wet (with H$_2$O) reforming produce synthesis gas [2]. The CO in synthesis gas is converted into pure hydrogen by water–gas shift reaction, however this hydrogen still contains enough CO to poison the catalyst. Among several processes the common feature is the high temperature operation due to the stable C—H bond of CH$_4$ that makes it very difficult to decompose. In the case of direct thermal decomposition of methane the formation of CO free hydrogen, carbon in the form of carbon nanofibres and carbon nanotube makes this process more interesting because these materials have lots of scientific and technological potential [3].

Among several catalysts, Fe, Cu and Ni based catalysts are found as a promising catalyst for methane decomposition reaction [4]. Recently, both molecular simulation and experimental results suggest that the bimetallic catalysts manifest unique catalytic properties in CNF and CNT growth. The bimetallic interaction of Ni and Fe are well documented in the literature [5–9]. Typically, such catalysts are composed of Al$_2$O$_3$ or other oxides as support. Muradov has attempted the pyrolysis of methane to produce CO$_2$ free hydrogen using alumina supported Fe$_2$O$_3$ and NiO (10 wt%) at 850 °C [10,11]. It is proposed that before reaching the steady state methane decomposition the oxide phase reduced to catalytically active metal and carbide phases followed by depletion of these active phases. While reviewing several factors controlling the activity of iron catalyst; the catalyst preparation, calcination temperature, and presence of bi-metallic sites (Ni–Fe) are most important to be focussed. It is reported that 650 °C is the highest temperature for attaining maximum conversion irrespective of Ni loading, however the maximum value of conversion increases with the increase in Ni content [12].

The development of novel materials is a fundamental focal point of chemical research which has been nurtured well in the last decades. Generally, impregnation, co-precipitation and sol–gel methods are widely used for the preparation of different supported catalysts. Co-precipitation reactions involve the simultaneous occurrence of nucleation, growth, coarsening and agglomeration processes. Impregnation is a method to

introduce appropriate active metal constitutions into the support. For supported catalyst, impregnation is widely used because of the simple method and easy dispersion of the active component on the surface of the supporter, which improves its utilization as a catalyst [13]. The sol–gel syntheses of inorganic nanoparticles have been studied extensively by several groups. Generally the hydrolysis of inorganic precursor and condensation of hydroxides are major steps to prepare the interconnected gelatinous material which after drying produces oxide nanoparticles [14]. Therefore the correlation between catalyst preparation method and the catalytic activity is always rewarding from fundamental and application point of view.

In this paper, we report the development of highly active unpromoted and nickel promoted Fe/Al$_2$O$_3$ catalyst for methane decomposition reaction. The catalysts are prepared by three different methods, e.g. impregnation, sol–gel and co-precipitation and calcined in two different temperatures i.e. at 500 °C and 800 °C temperatures. The catalysts are being characterized by BET, XRD, TPR, TGA techniques and catalytic activities were tested in the fixed-bed reactor. The spent catalysts have been characterized by TEM, XRD and TGA techniques. An attempt was taken to correlate the catalytic activity with the catalyst characterization results which might be useful to design efficient catalyst for methane decomposition reaction.

2. Materials and methods

2.1. Catalyst preparation

Analytical grades of iron nitrate [Fe(NO$_3$)$_3$·9H$_2$O; 98% pure purchased from Loba chemie®], nickel nitrate [Ni(NO$_3$)$_3$·6H$_2$O; 97% pure purchased from BDH Chemicals®], aluminium nitrate [Al(NO$_3$)$_3$·6H$_2$O; 97% pure purchased from BDH Chemicals®] and alumina [SA-6175; purchased from Norton®] were employed without further purification. The catalysts containing different loadings of Fe and Ni were prepared using the following three methods:

2.1.1. Impregnation method (Imp)

The wet-impregnation method was used to prepare the catalysts and the total Fe loading with all catalysts was fixed at 20 wt% with respect to Al$_2$O$_3$ support. In a typical wet-impregnation process, the solution having a stoichiometric amount of [Fe(NO$_3$)$_2$·9H$_2$O] was prepared using double distilled water. Afterwards respective supports were added to the solution with constant stirring at 85 °C. Then catalysts were dried at 120 °C for about 13 h, followed by calcination at 500 °C or 800 °C in atmospheric air for 3 h. To prepare 5 and 10 wt% Ni promoted Fe/Al$_2$O$_3$ catalyst, the co-impregnation of nitrate salts of the Fe and Ni with Al$_2$O$_3$ support was taken and the same procedure as described above was adapted.

2.1.2. Co-precipitation method (Cp)

To prepare Al_2O_3 supported Fe catalyst by co-precipitation method the stoichiometric amount of $[Fe(NO_3)_2 \cdot 9H_2O]$ and $[Al(NO_3)_3 \cdot 9H_2O]$ were added into double distilled water under constant stirring at 80 °C. Then 10% ammonia solution was added drop wise until pH 9 was reached in order to precipitate hydroxides from the solution. The precipitates were subsequently filtered and washed with distilled water and acetone to remove impurities. The precipitates were subjected to drying at 120 °C overnight and finally calcined at 500 °C or 800 °C for 3 h under atmospheric air. To prepare the Ni promoted Fe/Al_2O_3 catalyst. Fe metal loading was fixed at 20 wt%, while Ni metal loading was chosen by 5 and 10 wt% and the same procedure as mentioned above was adapted.

2.1.3. Sol–gel method

In a typical sol gel method alumina precursor i.e., Disperal P2, a water dispersible alumina (AlOOH, boehmite, 75% Al_2O_3, Sasol) having primary particle size of 5 nm was used. Moreover, Triton was employed as nonionic surfactant. In a 250 ml beaker 80 g water and 20 g Disperal P2 were stirred with a magnetic stirrer at room temperature for 1 h. Then 10 g Triton X100 are added and stirring is continued for another 30 min. The magnetic stirrer is now removed and a solution of 27 g $Fe(NO_3)_3 \cdot 9H_2O$ in 15 g water is added under mixing with the help of a plastic or Teflon spatula. The orange coloured gel is now shaped with the use of a big plastic syringe (50 ml). The opening diameter of the syringe is 2 mm. With the help of the syringe the gel is placed as 2 mm stripes on a big plate. The gel is dried over night at room temperature and then for 12 h at 90 °C. The calcination of 10 g of the sample was done with a tubular furnace with a heating rate of 1 K/min in a flow of air (150 ml/min) up to 500 °C or 800 °C with 3 h holding time at the applied temperature.

For the iron–nickel catalyst preparation the proper amount of nickel nitrate was added to the iron nitrate solution and the same procedure as above was used.

2.2. Catalyst characterization

2.2.1. X-ray diffraction characterization

Powdered X-ray diffraction (XRD) analysis of fresh and used catalyst was carried out using a Rigaku (Miniflex) diffractometer with a Cu Kα radiation operated at 40 kV and 40 mA. The scanning step and range of 2θ for analysis were 0.02° and 10–85° respectively. The raw data file of the instrument is analyzed by X'pert high score plus software. The peak intensity is measured and ASCII file is generated at granularity 8, bending factor 5, minimum peak significance 1, minimum peak width 0.40, maximum tip width 1 and peak base width 2 by minimum second derivatives. Further different phases with their scores are matched by JCPDS data bank and X'pert high score plus software. Finally, XRD is plotted after 5 point smoothing in Origin 6.0.

2.2.2. N_2 physisorption study

The specific surface area of the catalysts was determined from N_2 adsorption–desorption data at −196 °C using a Micromeritics Tristar II 3020 surface area and porosity analyzer. For each analysis, 0.3 g of catalyst was degassed at 300 °C for 3 h to remove moisture content from the catalyst surface as well as other adsorbed gases. Pore size distribution was calculated by BJH method.

2.2.3. Temperature programmed reduction (TPR)

The TPR measurements were completed on a chemisorption apparatus (Micromeritics Auto Chem II apparatus) using 70 mg for each sample. The samples were pretreated with high purity Argon (Ar) flowing at 150 °C for 30 min, followed by cooling to room temperature and then heating in a furnace up to 1000 °C with a constant heating rate of 10 °C/min using a H_2/Ar mixture at the flow rate of 40 mL/min (volume ratio, 10/90). The signal of H_2 consumption was monitored by a thermal conductivity detector (TCD).

2.2.4. Transmission electron microscopy (TEM) analysis

Transmission electron microscopy (TEM) measurements of spent samples were performed with a JEOL JEM-1400 transmission electron microscope operated at 120 kV accelerating voltage for in-depth analysis of the morphology of the nanostructured deposited carbon. For TEM analysis, the samples were first dispersed ultrasonically in ethanol at room temperature. Then, a few drops of the resulting suspension were put on a lacy carbon-coated Cu grid to take images.

2.2.5. Thermo-gravimetric analysis (TGA)

The quantitative analysis of coke deposition from 3 h reaction time on the surface of the spent catalysts was carried out by thermo-gravimetric analysis (TGA) in an air atmosphere using EXSTAR SII TG/DTA 7300 (Thermo-gravimetric/Differential) analyzer. 10–15 mg of the used catalyst was heated from room temperature to 800 °C at a heating rate of 20 °C /min under air flowing at 20 mL/min and loss of weight was measured.

2.3. Activity study of the catalyst

The methane decomposition reaction was carried out at atmospheric pressure in a 9.1 mm i.d. and 30 cm long stainless steel fixed-bed continuous-flow micro-reactor (PID Micromeritics) using 0.3 g of the catalyst. The reactor assembly contains single heating zone furnace and the reaction temperature was measured using a K-type thermocouple placed axially centred in the catalyst bed. The operating gas hourly space velocity was 5000 mL/h g_{cat}. The reactant gas was comprised of CH_4 and N_2 in the ratio of 1.5:1. Prior to the reaction, the catalyst, calcined at 500 °C and 800 °C was subjected to reduction at 500 °C and 700 °C respectively, using hydrogen gas at a flow rate of 40 mL/min for 90 min and the catalytic activity was studied in fixed reaction temperature of 700 °C. The effluent gases were analyzed by an online gas chromatograph (Shimadzu GC-2014) equipped with a thermal conductivity detector (TCD, using column (PP-Q). CH_4 conversion and hydrogen yield were calculated using the following formulae:

$$CH_4 \text{ Conversion}(\%) = \frac{CH_{4 \text{ in}} - CH_{4 \text{ out}}}{CH_{4 \text{ in}}} \times 100$$

$$\%\text{Yield of } H_2 : Y_{H_2} = \frac{\text{Moles of hydrogen produced}}{2 \times \text{Mole of } CH_4 \text{ in feed}} \times 100$$

3. Results and discussion

3.1. Pre-reaction characterization (20% Fe/Al₂O₃ catalyst)

3.1.1. X-ray diffraction (XRD)

XRD image and phase distribution of different catalyst samples prepared by co-precipitation, sol–gel and impregnation method are shown in (Fig. 1). The 20 wt% iron supported on alumina prepared by co-precipitation method had hercinite ($FeAl_2O_4$) mixed oxide phase (JCPDS card No. 34-0192). As preparation method changes from co-precipitation method to impregnation method, iron oxide phases hematite (JCPDS card No. 33-0664) and maghemite (JCPDS card No. 00-039-1346) were obtained. It is noticeable that impregnated catalyst samples calcined at a higher temperature have additional aluminium oxide phases (Corrundum, JCPDS card No. 00-046-01212) and alumina (JCPDS card No. 00-042-01468).

3.1.2. N₂-physisorption analysis

The surface area and porosity results of the samples prepared by three different methods and calcined at 500 °C and 800 °C are provided in Figs. S1 and S2 in Supporting Information as well as in Table 1. It is observed that samples prepared by sol–gel and co-precipitation methods have a higher surface area compared to the sample prepared by impregnation method. The samples prepared by sol–gel and co-precipitation methods have type-IV isotherm with H_2 hysteresis loop as depicted in Fig. S1) indicating the presence of mesopores. However, impregnated sample showed isotherm of type-II with H2 hysteresis loop. As reported in the literature, the H_2 hysteresis loop is due to capillary condensation [15]. The pore-size distribution results show that samples prepared using impregnation and co-precipitation methods have bigger pores compared to samples prepared by the sol–gel method. The higher surface area for the samples prepared by sol–gel as well as a co-precipitation method may be due to smaller crystallite sizes generated by homogeneous nucleation and growth process. After calcinations at 800 °C temperatures the surface area of the samples prepared by impregnation and co-precipitation method decreased, however the catalyst prepared by the sol–gel method retained its textural property. The BET isotherms for samples prepared by co-precipitation, impregnation and co-precipitation methods remain unchanged. The sintering of smaller particles to a bigger one for co-precipitated and impregnated samples might reduce the surface area. The samples prepared by the sol–gel method have $FeAl_2O_4$ phase as evidenced in the XRD results. The pore-size increases for the sample prepared
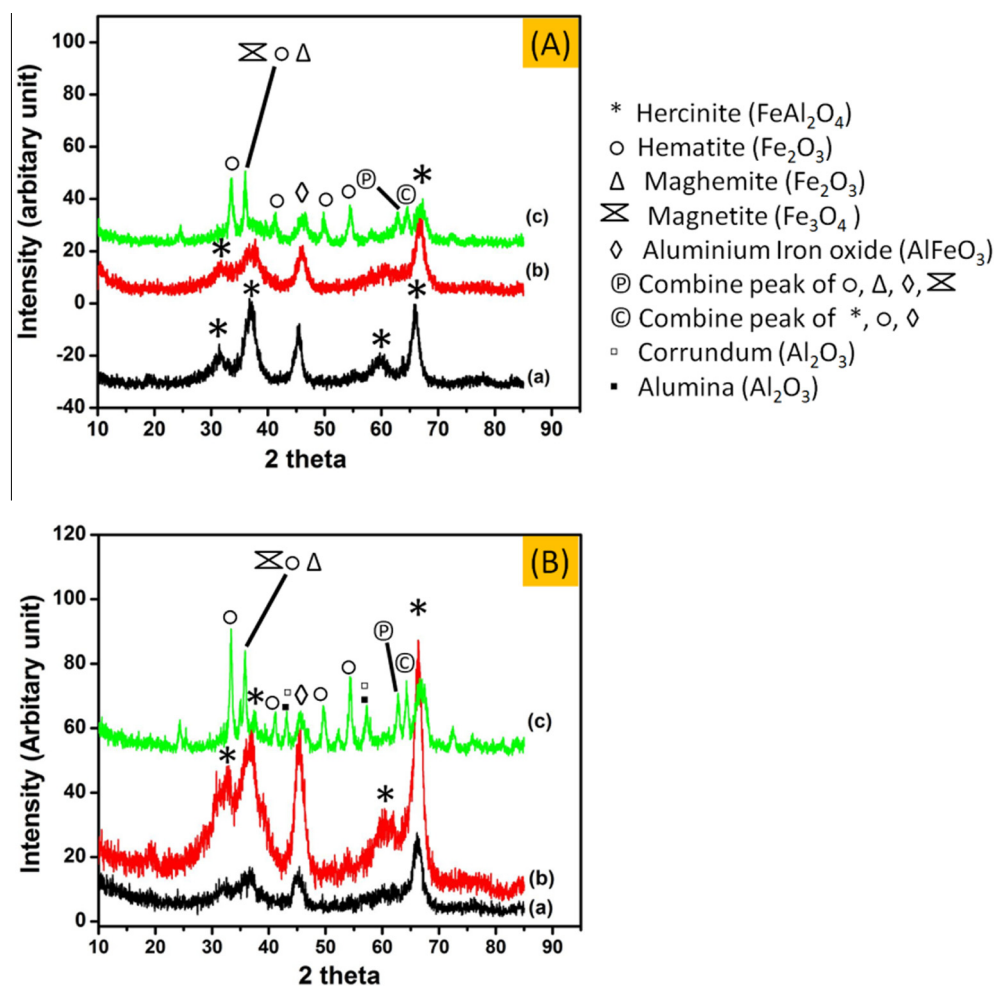

Figure 1 XRD pattern of 20% Fe/Al₂O₃ catalyst (A) calcined at 500 °C temperature (B) calcined at 800 °C temperature; prepared by (a) Co-precipitation method (b) sol–gel method (c) impregnation method.

Table 1 N_2 physisorption results for 20% Fe/Al_2O_3 catalyst.

Catalyst	Method	Calcination temperature (°C)	BET surface area (m^2/g)
20% Fe/Al_2O_3	Imp.	500	155
20% Fe/Al_2O_3	Sol–gel	500	208.9
20% Fe/Al_2O_3	Cp	500	237
20% Fe/Al_2O_3	Imp	800	95.5
20% Fe/Al_2O_3	Sol–gel	800	203.3
20% Fe/Al_2O_3	Cp	800	104.1

by impregnated and co-precipitation methods which may be due to some inter-particle pores.

3.1.3. Temperature programmed reduction (TPR)

The nucleation and size of the Fe oxide particle are expected to affect the chemical property of the catalyst. To investigate the interaction with the support matrix in different preparation methods the TPR experiments are carried out as shown in Fig 2. From a qualitative point of view two main reduction peaks with well defined maxima at ca 350–450 °C and 700–800 °C dominated in the TPR profile for most of the cases. The two well defined TPR peaks suggest a two step reduction of hematite to metallic iron through wüstite (FeO) and magnetite (Fe_3O_4) intermediate [16]. The reduction profile for the samples calcined at a higher temperature showed an interesting feature. The reduction profile did not change for the samples prepared by sol–gel and co-precipitation methods. However, the reduction peak at 700 °C for impregnated sample calcined at 800 °C shifted to a higher temperature. This is mainly due to the agglomeration of smaller crystallites during high temperature calcinations. It can be said that different type of Fe and Al containing phases which are present for the samples prepared by three different methods and varying calcination temperatures have different reduction profiles. For impregnation the interaction of iron oxide interacts with alumina which is supported by the XRD sharp peaks for iron oxide alone. For co-precipitated and sol gel method the probability of strong interaction between iron oxide and alumina is much higher
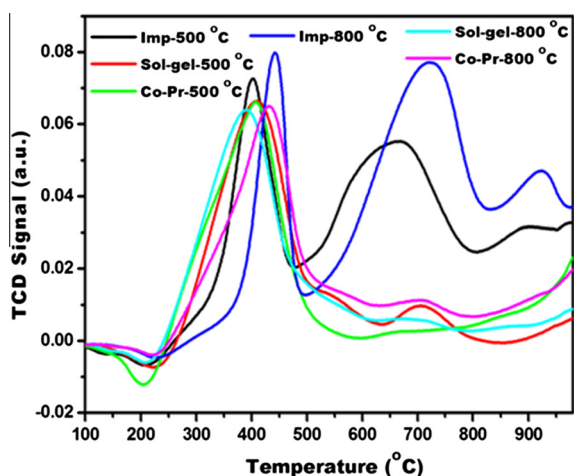
because aluminium hydroxide and oxyhydrates are much more reactive than gamma alumina. This means in this case we generate more spinel phases that are not reducible.

3.2. Catalytic activity results

The catalytic activity data for the Fe/Al_2O_3 catalyst prepared by three different methods i.e. impregnation, co-precipitation and sol–gel along with calcination at 500 °C and 800 °C temperatures are presented in Fig. 3a. The catalysts calcined at 500 °C showed a similar picture with an increase in activity during the first 60 min (TOS) with respect to methane conversion. After that a steady activity with a conversion of 60%, 50% and 45% for imp, sol gel and Cp, respectively were observed. Increasing calcination temperature to 800 °C led to the different behaviour of the catalysts. The impregnated sample calcined at 800 °C showed the same activity as for the calcined at 500 °C. It starts with lower activity around 55% conversion during the first 60 min but then conversion increases up to 60% though, the catalysts prepared by sol–gel and co-precipitation methods calcined at 800 °C found to be less active compared to the samples calcined at 500 °C. In addition, the conversion is decreasing with the increase in time on stream (TOS). While evaluating the catalyst performance in terms of hydrogen yield Fig. 3b, the similar trends were followed. The type of iron oxide species has a prominent role in the methane decomposition reaction. The more catalytic activity for the impregnated sample calcined at a high temperature may be due to low interaction with support and the presence of active iron oxide that was reducible as observed in TPR results. For the catalysts prepared by sol–gel and co-precipitation, the strong interaction of iron with alumina leads the formation of spinel which is inactive for the reaction. As reported by Motozuka et al. [17], the efficient CH_4 adsorptions as well as H_2 generation were observed on the disordered oxides, indicating an effectively dissociative adsorption.

They have shown using molecular orbital calculation analysis that activated oxygen atoms with dangling bonds in the disordered iron oxides affect the C–H dissociation of the adsorbate molecules (CH_4 or CH_3^*) and exhibit an efficient H_2 generation. However, oxygen atoms in the ordered lattice could not induce C–H dissociation.

3.3. Post reaction characterization

3.3.1. X-ray diffraction characterization

XRD diffractograms and phase distribution of spent catalysts prepared by co-precipitation, sol–gel and impregnation methods are shown in Fig. S3 in Supporting Information. It is found that during the reaction, major phase transitions occur.
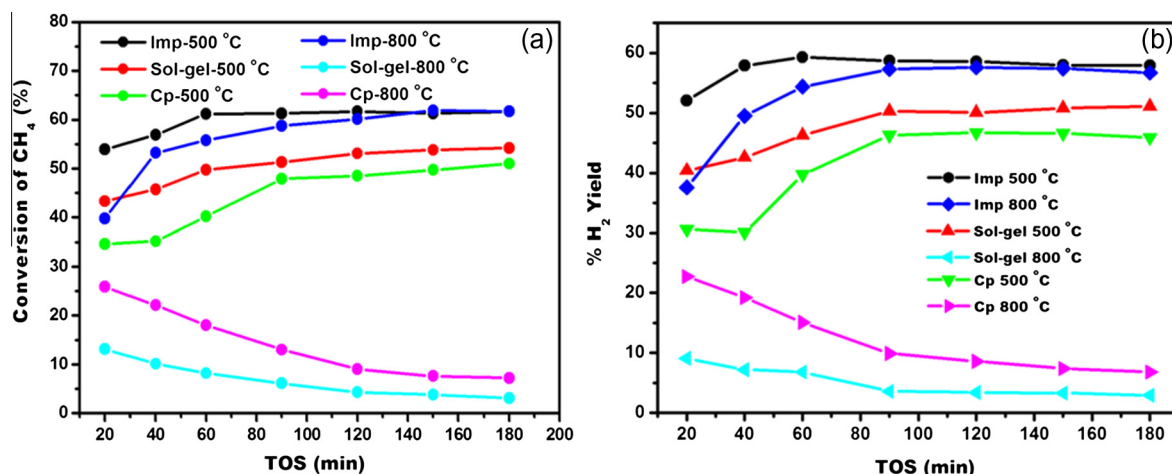

Figure 2 Temperature programmed reduction profile of 20% Fe/Al_2O_3 catalyst prepared by different methods and calcined at different temperature.

Figure 3 (a) Catalyst activity results of 20% Fe/Al_2O_3 catalyst for methane decomposition reaction. (methane/nitrogen 1.5/1, total flow rate 25 ml/min; space velocity 5000 ml/h g_{cat}); (b) catalyst activity results of 20% Fe/Al_2O_3 catalyst for methane decomposition reaction in terms of H_2 yield (methane/nitrogen 1.5/1, total flow rate 25 ml/min; space velocity 5000 ml/h g_{cat}).
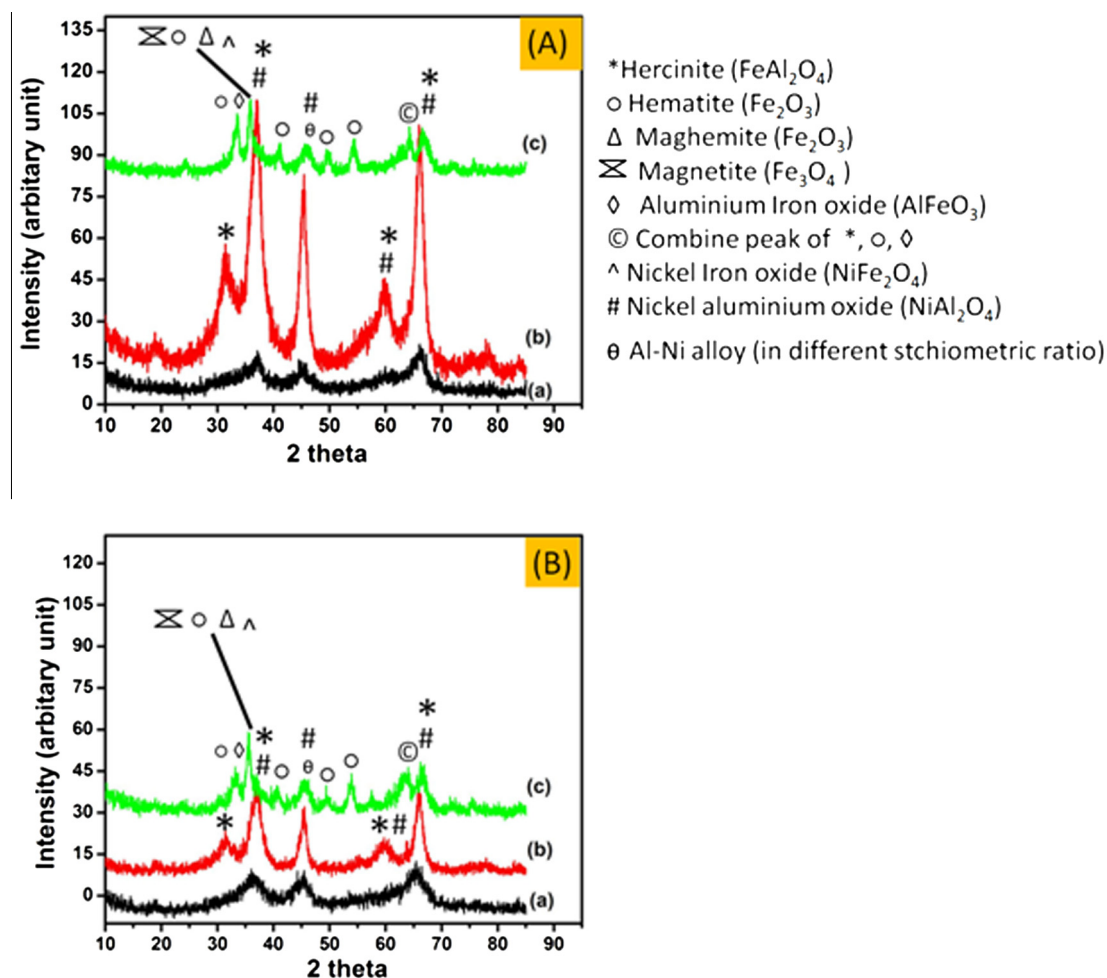

Figure 4 XRD pattern of (A) 20% Fe–5% Ni–Al_2O_3 calcined at 500 °C (B) 20% Fe–10% Ni–Al_2O_3 calcined at 500 °C; prepared by (a) co-precipitation method (b) sol–gel method (c) impregnation method.

In comparison with fresh catalyst, it is found that in fresh catalysts different iron oxide and mixed iron oxide phases are prominent. After reaction, Fe, Fe–Al Alloy (JCPDS card No. 00-033-0020) and metal carbide Fe_3C (JCPDS card No. 00-035-0772 and 00-034-0001) and Al_4C (JCPDS card No. 00-035-0799) phases are prominent in the spent catalysts.

Table 2 N$_2$ Physisorption results for 20% Fe–Ni/Al$_2$O$_3$ catalyst.

Catalyst	Method	Calcination temperature (°C)	BET surface area (m^2/g)
5% Ni + 20% Fe/Al	Imp.	500	147.7
5% Ni + 20% Fe/Al	Sol–gel	500	163.1
5% Ni + 20% Fe/Al	Cp	500	215.3
10% Ni + 20 Fe/Al	Imp.	500	140.6
10% Ni + 20 Fe/Al	Sol–gel	500	151.2
10 Ni + 20 Fe/Al	Cp	500	248.8

Increasing calcination temperature to 800 °C increases the intensity of XRD reflexes due to the increase of the crystallinity. The sol–gel and co-precipitation sample had hercinite as dominant phase, both in fresh and used catalysts. The spent impregnated catalyst calcined at 800 °C showed the presence of more iron carbides as mentioned before.

3.3.2. Transmission electron microscopy (TEM) characterization

In general, the growth of carbon nanofibres with a filamentous structure is obtained from the carbon deposition during methane decomposition as depicted in Fig. S4 in Supporting Information for impregnated catalysts. The Fe metal particle was always present at the tip of carbon nanofibre as observed in TEM image. The lengths of carbon nanofibre were close to 30 nm and diameter of iron particle was 20 nm as depicted in Fig. S4. The carbon atoms generated due to decomposition of methane present in the metal surface diffuse to the other side of the metal particle and precipitate as graphite layer [18]. For steady decomposition of methane, the balance between the decomposition rate of methane to carbon and hydrogen atom and rate of diffusion of carbon atoms over the metal particle is required.

3.3.3. Thermal gravimetric analysis (TGA)

The TGA profile of the used catalyst is shown in Fig. S5a and b. The temperature of the oxidation of carbon nanofibre is in the range of 500–700 °C. The impregnated sample had maximum weight loss (Supporting Information) and the loss is at a higher temperature, which clearly indicates formation of large amounts of carbon nanofibre after methane decomposition reaction on the catalyst surface.

3.4. Effect of promoter

In order to enhance the catalytic activity the Ni promoted Fe/Al$_2$O$_3$ catalysts were prepared. As the un-promoted catalyst had higher activity in the samples calcined at 500 °C temperature, so for the Ni promoted catalysts with different loading (5 wt% and 10 wt%) were prepared at 500 °C calcined temperature.

3.4.1. Pre-reaction characterization

3.4.1.1. X-ray diffraction characterization. The phase distribution of Ni promoted catalyst system is very similar to that of unpromoted except that it has nickel iron oxide, nickel aluminium oxide (JCPDS card No. 00-010-0339) and Al-Ni (JCPDS card No. 00-044-1188) alloy in different stoichiometric ratios. The nickel based catalyst prepared by co-precipitation method has nickel aluminium oxide whereas catalyst prepared

by the sol–gel method has both nickel aluminium oxide and intense hercinite phase. Nickel promoted iron impregnated samples have additional iron oxide (hematite), maghemite, aluminium iron mixed oxide and nickel iron mixed oxide (NiFe$_2$O$_4$) phases Fig. 4.

3.4.1.2. N$_2$-physisorption studies. To see the effect of the Ni promotion of the textural property of Fe/Al$_2$O$_3$ catalyst the N$_2$ Physisorption studies are carried out. As observed from N2-physisorption studies (Figs. S6 and S7 in Supporting Information and Table 2) there is a change in isotherm profile and pore size distribution in nickel promoted Fe/Al$_2$O$_3$ catalyst. For the samples prepared by the sol–gel method the addition of nickel does not show an effect on the pore size distribution. The formation of NiFe$_2$O$_4$ phase as observed in XRD studies is responsible for unimodal pore-size distribution. The pore size distribution is mostly affected by the addition of nickel during preparation of the catalyst by co-precipitation method. As the isoelectric pH of NiO, Al$_2$O$_3$ and Fe$_2$O$_3$ are different, therefore the formation of hydroxides are extremely complicated while preparing by co-precipitation method. As evidenced in the literature, it is complicated, whether the as-prepared precursor is a single-phase solid solution or multi-phase one [19]

3.4.1.3. Temperature programmed reduction (TPR). For Ni promoted Fe/Al$_2$O$_3$ catalyst there are peaks at 350 °C, 650 °C, 800 °C, and 950 °C temperature as shown in Fig. 5 which are in the range of those of NiO and Fe$_2$O$_3$.
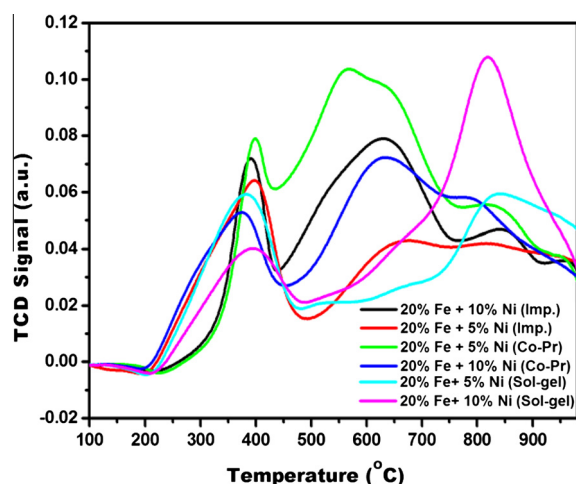

Figure 5 Temperature programmed reduction profile of 20% Fe–Ni/Al$_2$O$_3$ catalyst prepared by different methods.
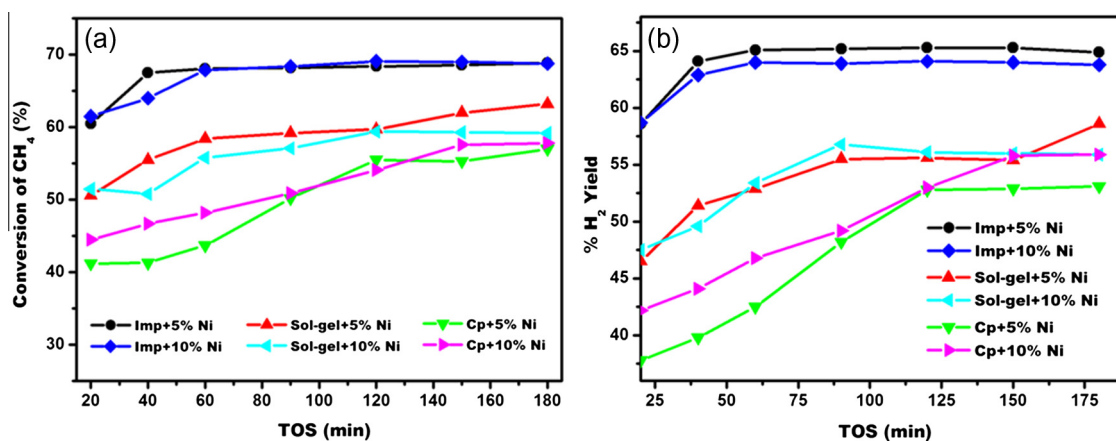
Figure 6 (a) Methane conversion versus time on stream for Ni-promoted Fe/Al$_2$O$_3$ catalysts calcined at 500 °C activity results of 20% catalyst for methane decomposition (methane/nitrogen 1.5/1, total flow rate 25 ml/min; space velocity 5000 ml/h g$_{cat}$); (b) hydrogen yield vs time on stream for Ni promoted 20% Fe/Al$_2$O$_3$ catalyst (methane/nitrogen 1.5/1, total flow rate 25 ml/min; space velocity 5000 ml/h g$_{cat}$).

Interestingly the presence of NiFe$_2$O$_4$ phase was more in the case of nickel promoted catalyst prepared by impregnation method as evidenced in XRD study. The hydrogen consumption peak at 950 °C is mainly due to reduction of magnetite to metallic iron. The third reduction peak is due to the transformation of Ni–FeO solid solution into Fe–Ni alloy and α-Fe [4]. Therefore, higher activity for nickel promoted catalyst while synthesized by the impregnation method is well justified by TPR results as a catalyst is easily reducible. Addition of Ni here has an effect on the reduction temperature compared to unpromoted catalysts.

3.4.2. Catalytic activity results

The effect of Ni promoter addition on the activity of the Fe/Al$_2$O$_3$ catalyst for methane decomposition reaction has been depicted in Fig. 6a and b. As the calcination at 800 °C leads to low conversions and deactivation catalysts only after calcination at 500 °C were measured in decomposition of methane. It is observed that for all the catalysts irrespective of the preparation method, there is an increase of 10% of methane conversion and hydrogen yield after nickel addition. Pure nickel is a very active catalyst, exhibiting the lowest initial methane decomposition temperature of all catalysts tested. Unfortunately, it also gets deactivated very fast at lower temperatures [12]. In the present case addition of small amounts of Ni to Fe/Al$_2$O$_3$ catalyst not only considerably improved the activity, but also prevented the substantial reduction in activity exhibited by pure Ni catalysts. Chesnokov and Buyanov compared the carbon diffusion co-efficient in Ni and Fe and found that the diffusion of carbon atoms in iron is 3 orders of magnitude higher than that in the nickel phase [20]. Modification of the Fe with Ni doping may decrease the carbon atom formation rate. Thus, the balance between the carbon atom formation, diffusion and precipitation is maintained, leading to great improvement of the stability of the catalyst in the reaction [20,21]. In addition, the type of the carbon plays an important role. The generation of graphitic carbon type on the surface of the catalyst causes fast deactivation. Doubling the Ni-loading from 5% to 10% slightly increases the conversion.

3.4.3. Post reaction characterization

3.4.3.1. Transmission electron microscopy (TEM) characterization.
The formation of carbon nanofibres with a diameter of 16–20 nm is observed for the nickel promoted Fe/Al$_2$O$_3$ catalyst after the reaction (Fig. S8 in Supporting Information). As discussed earlier the rate of carbon formation, diffusion and precipitation should be equal for high catalytic activity of methane decomposition. The controlled deactivation and increased rate of methane decomposition in the nickel promoted catalyst implies that carbon does not accumulate on the exposing face of metal particle responsible for methane adsorption and dissociation. It is well reported in the literature that, on the basis of the deposition–diffusion–precipitation mechanism, metal particles control the carbon growth [18].

3.4.3.2. Thermo gravimetric analysis (TGA) characterization.
The TGA profile of used catalysts is shown in Fig. S9 in Supporting Information. For all the nickel promoted samples the weight loss is at a higher temperature which strongly argues that carbon deposition is maximized (Supporting Information) for all samples irrespective of preparation procedure.

4. Conclusion

In conclusion, a thorough study demonstrates the catalyst preparation procedure has a significant role controlling the catalytic activity for methane decomposition reaction. The impregnation method was the most effective to sustain the catalytic activity, even at a higher calcination temperature. As observed from XRD mostly Fe-mixed oxide phases are responsible for the dissociative chemisorptions of methane. The TPR profile shows iron phases that are easily reducible compared to co-precipitate and sol gel which forms an iron–alumina spinel that is difficult to reduce. Addition of Ni to iron supported alumina catalysts enhances the methane conversion and H$_2$ yield to 10%. The formation of carbon nanotube was markedly changed as observed from TEM studies. The TGA characterization shows the amount of carbon deposition varies with preparation method, calcination temperature and Ni promotion.

Acknowledgement

Appendix A. Supplementary data

Supplementary data associated with this article can be found, in the online version, at http://dx.doi.org/10.1016/j.jscs.2016.05.001.

References

[1] M. Friedrich, D. Teschner, A. Knop-Gericke, M. Armbrüster, Surface and subsurface dynamics of the intermetallic compound ZnNi in methanol steam reforming, J. Phys. Chem. C 116 (2012) 14930–14935.

[2] T. Wang, Y. Li, C. Wang, X. Zhang, L. Ma, C. Wu, Synthesis gas production with NiO−MgO/Γ-Al2O3/cordierite monolithic catalysts in a pilot-scale biomass-gasification-reforming system, Energy Fuels 25 (2011) 1221–1228.

[3] N. Shah, D. Panjala, P. Huffman, Hydrogen production by catalytic decomposition of methane, Energy Fuels 15 (2001) 1528–1534.

[4] G. Wang, Y. Jin, G. Liu, Y. Li, Production of hydrogen and nanocarbon from catalytic decomposition of methane over a Ni–Fe/Al2O3 catalyst, Energy Fuels 27 (2013) 4448–4456.

[5] M. Pudukudy, Z. Yaakob, M. Mohammad, B. Narayanan, K. Sopian, Renewable hydrogen economy in Asia – opportunities and challenges: an overview, Renewable Sustainable Energy Rev. 30 (2014) 743–757.

[6] M. Pudukudy, Z. Yaakob, Methane decomposition over Ni, Co and Fe based monometallic catalysts supported on sol gel derived SiO2 microflakes, Chem. Eng. J. 262 (2015) 1009–1021.

[7] M. Pudukudy, Z. Yaakob, Z.S. Akmal, Direct decomposition of methane over SBA-15 supported Ni, Co and Fe based bimetallic catalysts, Appl. Surf. Sci. 330 (2015) 418–430.

[8] M. Pudukudy, Z. Yaakob, Z.S. Akmal, Direct decomposition of methane over Pd promoted Ni/SBA-15 catalysts, Appl. Surf. Sci. 353 (2015) 127–136.

[9] M. Pudukudy, Z. Yaakob, M.S. Takriff, Methane decomposition over Pd promoted Ni/MgAl2O4 catalysts for the production of COx free hydrogen and multiwalled carbon nanotubes, Appl. Surf. Sci. 356 (2015) 1320–1326.

[10] N.Z. Muradov, CO2-free production of hydrogen by catalytic pyrolysis of hydrocarbon fuel, Energy Fuels 12 (1998) 41–48.

[11] A.S. Al-Fatish, A.A. Ibrahim, A.H. Fakeeha, M.A. Soliman, M.R.H. Siddiqui, A.E. Abasaeed, Coke formation during CO2 reforming of CH4 over alumina-supported nickel catalysts, Appl. Catal. A Gen. 364 (2009) 150–155.

[12] J. Chen, Y. Li, Y. Ma, Y. Qin, L. Chang, Formation of bamboo-shaped carbon filaments and dependence of their morphology on catalyst composition and reaction conditions, Carbon 39 (2001) 1467–1475.

[13] H. Liu, Y. Zhou, Y. Zhang, L. Bai, M. Tang, Effect of preparation processes on catalytic performance of PtSnNa/ZSM-5 for propane dehydrogenation, Ind. Eng. Chem. Res. 48 (2009) 5598–5603.

[14] C. Santra, S. Rahman, S. Bojja, O. James, D. Sen, S. Maity, K.A. Mohanty, S. Mazumderd, B. Chowdhury, Barium, calcium and magnesium doped mesoporous ceria supported gold nanoparticle for benzyl alcohol oxidation using molecular O2, Catal. Sci. Technol. 3 (2013) 360–370.

[15] S. Rahman, C. Santra, R. Kumar, J. Bahadur, A. Sultana, R. Schweins, D. Sen, S. Maity, S. Mazumdar, B. Chowdhury, Highly active Ga promoted Co-HMS-X catalyst towards styrene epoxidation reaction using molecular O2, Appl. Catal. A Gen. 482 (2014) 61–68.

[16] M.A. Ermakova, D.Y. Ermakov, Ni/SiO2 and Fe/SiO2 catalysts for production of hydrogen and filamentous carbon via methane decomposition, Catal. Today 77 (2002) 225–235.

[17] S. Motozuka, M. Tagaya, T. Ikoma, M. Morinaga, T. Yoshioka, J. Tanaka, Efficient methane conversion to hydrogen by the force-activated oxides on iron particle surfaces, J. Phys. Chem. C 117 (2013) 16104–16118.

[18] Y. Shen, A.C. Lua, Synthesis of Ni and Ni–Cu supported on carbon nanotubes for hydrogen and carbon production by catalytic decomposition of methane, Appl. Catal. B Environ. 164 (2015) 61–69.

[19] B.M. Reddy, B. Chowdhury, P.E. Reddy, A. Fernandez, X-ray photoelectron spectroscopy study of V2O5 dispersion on a nanosized Al2O3-TiO2 mixed oxide, Langmuir 17 (2001) 1132–1137.

[20] V.V. Chesnokov, R.A. Buyanov, The formation of carbon filaments upon decomposition of hydrocarbons catalysed by iron subgroup metals and their alloys, Russ. Chem. Rev. 69 (2000) 623–638.

[21] R.J. Wrobel, A. Hełminiak, W. Arabczyk, U. Narkiewicz, Studies on the kinetics of carbon deposit formation on nanocrystalline iron stabilized with structural promoters, J. Phys. Chem. C 118 (2014) 15434–15439.